

Graph-Dictionary Signal Model for Sparse Representation of Multivariate Data

William Cappelletti, Pascal Frossard
LTS4, EPFL, Lausanne, Switzerland

Abstract—Representing and exploiting multivariate signals requires capturing relations between variables, which we can represent by graphs. Graph dictionaries allow to describe complex relational information as a sparse sum of simpler structures, but no prior model exists to infer such underlying structure elements from data. We define a novel Graph-Dictionary signal model, where a finite set of graphs characterizes relationships in data distribution as filters on the weighted sum of their Laplacians. We propose a framework to infer the graph dictionary representation from observed node signals, which allows to include a priori knowledge about signal properties, and about underlying graphs and their coefficients. We introduce a bilinear generalization of the primal-dual splitting algorithm to solve the learning problem. We show the capability of our method to reconstruct graphs from signals in multiple synthetic settings, where our model outperforms popular baselines. Then, we exploit graph-dictionary representations in an illustrative motor imagery decoding task on brain activity data, where we classify imagined motion better than standard methods relying on many more features. Our graph-dictionary model bridges a gap between sparse representations of multivariate data and a structured decomposition of sample-varying relationships into a sparse combination of elementary graph atoms.

I. INTRODUCTION

Multivariate signals represent joint measurements from multiple sources, and commonly arise in different fields. They might represent electrical potentials generated by brain activity, as well as stock values in the financial market, temperatures across weather stations, or traffic measurements at road junctions. Generally, we study these signals to characterize the system on which we measure them; for instance, to classify brain activity for motor imagery analysis, or to capture hidden relationships between variables. We are interested in effective representations that can provide an explanation of the relational information between different sample variables, to identify the role of each source, and describe the distribution of their outcomes. Graphs provide a natural representation of structured data with pairwise relationships, described by *edges* between *nodes*, however, these relationships are often hidden, and we must infer them from data.

Many multivariate systems are governed by complex instantaneous dynamics, which can vary for every data sample, but which might be modeled as the joint effect of simpler structures. For instance, when measuring the electrical brain activity of a subject, we capture ionic currents resulting from multiple synaptic processes happening at the same time—like vision processing and motor activity. Furthermore, the contribution of each simpler dynamic is often sparse in time; for example on traffic measurements, where commuters drive

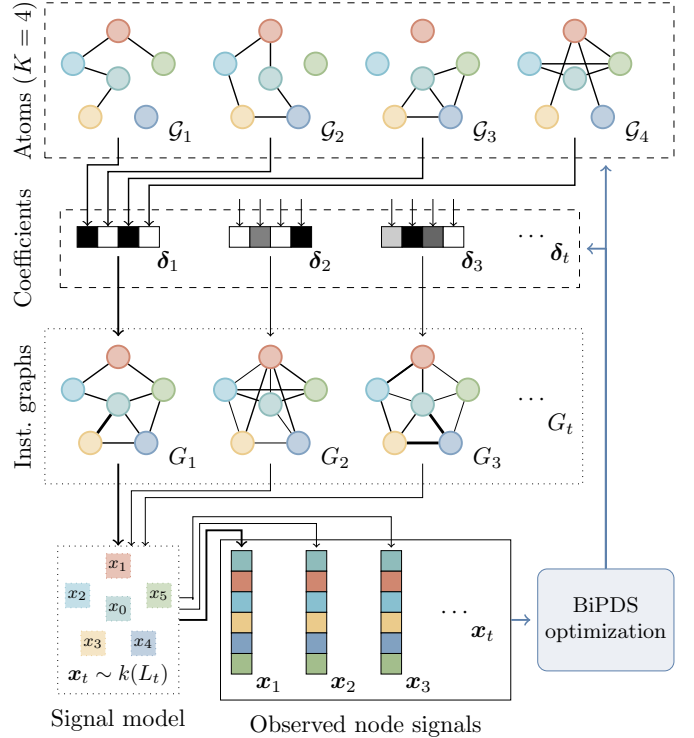


Fig. 1. Representation of our novel graph-dictionary signal model. Solid black arrows illustrate the generative process, where coefficients δ_t mix atoms $\mathcal{G}_1, \dots, \mathcal{G}_K$ from the dictionary to give instantaneous graphs G_t , whose Laplacians L_t characterize the signal model from which signals \mathbf{x}_t are sampled. In particular, the **thick** arrows follow the generation of \mathbf{x}_1 . Along **blue** lines we see the inverse problem, which jointly learns atoms and coefficients from observed signals using our Bilinear Primal Dual Splitting algorithm.

during specific hours on their usual path, which might overlap with the mobility patterns of service vehicles, or tourist cars.

We approach this representation learning problem through *dictionary learning* [1]. This framework aims to recover a finite set of atoms, called a *dictionary*, that can encode data through sparse coefficients. We introduce a novel Graph-Dictionary signal model, *GraphDict* in short, to jointly address the representation and the structure learning problems. Following the *Graph Structure Learning* literature [2, 3], we use signal models to link each N -variate signal sample $\mathbf{x}_t \in \mathbb{R}^N$ to an underlying *instantaneous* graph G_t . Our novel approach, illustrated in Figure 1, uses a dictionary of graphs to characterize each G_t as the linear combination of K graph atoms $\mathcal{G}_1, \dots, \mathcal{G}_K$ with respective coefficients $\delta_t \in [0, 1]^K$. The coefficient vector corresponding to each sample provides an

embedding which is inherently explainable. More precisely, each entry describes the contribution of the corresponding graph atom, with edges defining instantaneous relationships that generate the observed signal. Our objective function jointly characterizes atoms and coefficients, and its optimization requires a novel generalization of the Primal-Dual Splitting algorithm, which we define by leveraging the adjoint functions of a bilinear operator [4].

We present a series of experiments to test the capabilities of our model. In two experiments on synthetic data, we show that GraphDict outperforms literature baselines in reconstructing instantaneous graphs from signals. Finally, we exploit the sparse representations given by GraphDict coefficients in an exploratory downstream classification task consisting in motor imagery decoding on brain activity data. We show that with few features on three connectivity atoms identified by our model, we classify imagined motion better than brain-state models from the neuroscience literature.

Our main contributions are the following:

- **Graph signal model.** We introduce *GraphDict*, a novel probabilistic model that defines multivariate signal distributions with graph dictionaries. We formulate signal representation learning as a maximum a posteriori estimate which allows for domain-specific priors on both the graph structures and the contributions of each dictionary atom.
- **Optimization algorithm.** We propose a novel bilinear generalization of the Primal-Dual Splitting algorithm to jointly learn edge weights of dictionary atoms and their mixing coefficients.
- **Practical implementation.** We illustrate some specific loss functions that include common hypotheses from graph structure learning and sparse representations, and we derive their optimization steps.
- **Performance Evaluation.** We present three experiments to investigate the ability of GraphDict’s declinations to reconstruct instantaneous graphs and provide helpful and explainable representations. Our model can reliably reconstruct instantaneous graphs on synthetic data, and its sparse coefficients’ representation outperforms established methods in an exploratory downstream classification task on motor imagery decoding.

The proposed graph-dictionary signal model provides a flexible tool to reconstruct relationships between variables in multivariate data, and decompose them in atomic graphs. The sparse representation corresponding to the network-atoms coefficients is useful in downstream tasks, and explicitly relates feature learning to relational information.

II. RELATED WORK

Learning graph dictionaries is a very recent trend, and multiple works [5, 6, 7, 8] address this problem starting from actual graph observations, while our framework only requires node signals. Methods based on optimal transport use different graph distances to learn dictionaries from unaligned graphs. Vincent-Cuaz et al. [5] propose an online learning method based on Gromov-Wasserstein (GW) Discrepancy, and

Liu et al. [6] expand this framework to be more robust to graph perturbations. Zeng et al. [7] propose a non-linear graph dictionary learning algorithm, and they formulate the problem from a generative perspective with a Fused GW Mixture Model, which combines optimal transport and kernel estimation. Das and Isufi [8] use tensor decomposition to identify a limited number of *key mode graphs*, equivalent to dictionary atoms, that can explain a temporal network, and whose linear combination represents its evolution. Furthermore, they use an alternating algorithm to optimize the mode graphs and the temporal factor variables, which may be suboptimal

To the best of our knowledge, the only previous work that links signals to graph dictionaries is from Thanou et al. [9], who suggest learning dictionaries of structured graph kernels from signals. They observe signals over a predefined graph, and the atoms of their dictionary represent different graph filters on the edges of such network. Our work, on the other hand, does not define the atoms as subgraphs of a known network, but learns edges from scratch, resulting in greater flexibility to capture complex dynamics. Still, our probabilistic approach allows introducing further regularization terms, and in Section VI we explain how to encompass the settings of Thanou et al. [9]. The recent paper from Karaaslanli and Aviyente [10] addresses a similar problem as they infer a multiview graph model from node signals, where each view is a perturbed version of an underlying consensus graph. Compared to our graph dictionary formulation, they learn a single recurrent structure—namely the consensus graph—of which views are “small” perturbations, while we allow more flexibility in the topologies on which signals are observed by inferring multiple atoms, which provide instantaneous graphs through linear combinations.

Another line of work that we cover with our Graph-Dictionary signal model consists in signal clustering and graph learning. In fact, we can see each cluster as an atom of a dictionary, with signal coefficients providing a vector encoding of cluster assignments. Maretic et al. [11], and Maretic and Frossard [12] propose Graph Laplacian Mixture Models (GLMM) in which precision matrices of the signals’ distribution depend on some function of the graph Laplacians. Similarly, Araghi et al. [13] design an algorithm for signals clustering and graph learning called *K*-Graphs, which refines assignments and graph estimation by expectation-maximisation. Both methods rely on a Gaussian assumption on the signal distribution, but while the latter model enforces hard assignments, like the *K*-means algorithm, GLMM performs soft clustering, by estimating the probability that a sample belongs to each cluster. Still, clustering methods need a significant separation between the underlying distributions; in graph signal models, this means they might struggle to discriminate samples if the underlying networks share multiple edges. Furthermore, they cannot capture continuous changes which can arise in more structured data such as multivariate time series.

III. GRAPH-DICTIONARY SIGNAL MODEL

In this section, we introduce *GraphDict*, our novel Graph-Dictionary signal model, and we describe the corresponding

representation learning problem.

A. Graphs and Signals

Our data $\mathbf{X} \in \mathbb{R}^{T \times N}$ represent a set of T signals of dimension N . For each $t \in T$ we observe a multivariate signal $\mathbf{x}_t \in \mathbb{R}^N$ on the nodes of a graph $G_t = (N, \mathbf{w}_t)$ whose edges $E \subset N \times N$ and corresponding weights $\mathbf{w}_t \in \mathbb{R}_+^E$ are unknown. Each edge $(i, j)_t$ describes a relation between signal outcomes x_{ti} and x_{tj} on nodes i and j for sample t , with a strength proportional to its weight w_{tij} . We focus on undirected graphs with nonnegative weights, which we represent as vectors $\mathbf{w} \in \mathbb{R}_+^{N(N-1)/2} = \mathbb{R}_+^E$.

Graph Signal Processing [14] provides us tools to understand the link between signals and the networks on which we observe them. One of its most important tools is the *combinatorial Laplacian* \mathbf{L} of a graph, which is defined as the difference between the diagonal matrix of node degrees and the adjacency matrix. Expressing it as a function of vectorized weights \mathbf{w} , the Laplacian is a linear operator from $\mathbb{R}_+^E \rightarrow \mathbb{R}^{N \times N}$:

$$[\mathbf{L}\mathbf{w}]_{ij} = \begin{cases} -w_{(i,j)} & i \neq j, (i,j) \in E, \\ \sum_{k:(i,k) \in E} w_{(i,k)} & i = j, \\ 0 & \text{otherwise.} \end{cases} \quad (1)$$

Of particular interest is the eigendecomposition of the Laplacian $\mathbf{L} = \mathbf{U}\mathbf{\Lambda}\mathbf{U}^\top$, with $\mathbf{\Lambda}$ the diagonal matrix of eigenvalues $\lambda_1 = 0 \leq \dots \leq \lambda_N$. We define the *Graph Fourier Transform* of a signal \mathbf{x} as the projection on the eigenbasis $\hat{\mathbf{x}} = \mathbf{U}\mathbf{x}$, and noting that eigenvectors are invariant signals, we introduce *graph frequencies* as the corresponding eigenvalues. We can finally define graph filters k as functions acting in the graph frequency domain [15], and represent them as

$$k(\mathbf{L}) = \mathbf{U}k(\mathbf{\Lambda})\mathbf{U}^\top. \quad (2)$$

B. Probabilistic Signal Model

We propose a model for multivariate data where the state of the system at each sample t is described by an underlying *instantaneous* graph G_t , given by a linear combination of K networks, which constitute the *atoms* of a *dictionary* of graphs. Our underlying hypothesis is that many complex systems can be described as the superposition of simpler recurring patterns.

Each N -variate sample signal $\mathbf{x}_t \in \mathbb{R}^N$ arises from a graph filter $k(\mathbf{L}_t)$ defined on the instantaneous Laplacian \mathbf{L}_t , applied to a random vector $\boldsymbol{\eta}_t \in \mathbb{R}^N$. This formulation provides much freedom to model complex systems, since by fixing k we are able to focus on specific properties that the signals \mathbf{x}_t display on the graph G_t , while allowing for great flexibility in the topology of the latter. For instance, we can consider iid multivariate white noise $\boldsymbol{\eta}_t \sim \mathcal{N}(\mathbf{0}, \mathbf{I}_N)$, so that

$$\mathbf{x}_t = k(\mathbf{L}_t)\boldsymbol{\eta}_t \sim \mathcal{N}(\mathbf{0}, k^2(\mathbf{L}_t)). \quad (3)$$

We define each instantaneous graph G_t through coefficients $\boldsymbol{\delta}_t \in [0, 1]^K$ and edge weights of each atom $\mathbf{w}_k \in \mathbb{R}_+^E$. We jointly represent the graph dictionary as the matrix $\mathbf{W} = [\mathbf{w}_1^\top, \dots, \mathbf{w}_K^\top] \in \mathbb{R}_+^{K \times E}$, whose rows identify atoms,

and we express instantaneous Laplacians as a bilinear form of coefficients $\boldsymbol{\delta}_t$ and weights \mathbf{W} as follows

$$\mathbf{L}_t = \mathbf{L}(\boldsymbol{\delta}_t, \mathbf{W}) = \sum_k \delta_{tk} \mathbf{L}_{\mathbf{w}_k} \in \mathbb{R}^{N \times N}. \quad (4)$$

Conditionally to this graph-dictionary formulation, the signal distribution P_x is characterized by $\boldsymbol{\delta}_t$ and \mathbf{W} . In this work, we assume that atom weights and coefficients are independent, meaning that structure and appearance do not influence each other. In this way, we can split the joint PDF in

$$P(\mathbf{X}, \mathbf{W}, \boldsymbol{\Delta}) = P_w(\mathbf{W})P_c(\boldsymbol{\Delta})P_x(\mathbf{X} | \mathbf{W}, \boldsymbol{\Delta}), \quad (5)$$

where P_w and P_c are the prior distributions of weights and coefficients respectively, and we gather all coefficients $\boldsymbol{\delta}_t$ in the rows of the matrix $\boldsymbol{\Delta} \in [0, 1]^{T \times K}$.

C. Representation Learning Problem

With the characterization of signal distribution with the graph dictionary and coefficients from Equation (5), we can define the representation learning problem as a maximum a posteriori (MAP) objective. Observing data $\mathbf{X} \in \mathbb{R}^{T \times N}$, we aim to find graph-dictionary weights \mathbf{W} and coefficients $\boldsymbol{\Delta}$ as the minimizers of the corresponding negative log-likelihood

$$\arg \min_{\mathbf{W}, \boldsymbol{\Delta}} \ell_w(\mathbf{W}) + \ell_c(\boldsymbol{\Delta}) + \ell_x(\mathbf{X}, \mathbf{W}, \boldsymbol{\Delta}), \quad (6)$$

where ℓ_w , ℓ_c , and ℓ_x are the negative logarithms of P_w , P_c , and P_x respectively.

This formulation leaves great flexibility for ℓ_w , ℓ_c , and ℓ_x which can enforce structure and domain-specific properties on atoms weights, coefficients, and signals respectively. While such priors are driven by the application, in Section IV we present a general algorithm to solve Equation (6) for \mathbf{W} and $\boldsymbol{\Delta}$. In Section V, we illustrate a practical example based on common assumptions, that we use in our experiments of Section VI.

IV. BILINEAR PRIMAL-DUAL SPLITTING ALGORITHM

To find a solution to the MAP objective (6) we propose Algorithm 1, a generalization of the Primal-Dual Splitting (PDS) algorithm by Condat [16]. Supposing that we can rearrange ℓ_w, ℓ_c from Equation (6) into a sum of Lipschitz-differentiable and proximable functions—denoted by f and g respectively, and separable in \mathbf{W} and $\boldsymbol{\Delta}$ —we can rewrite our optimization problem as

$$\arg \min_{\mathbf{W}, \boldsymbol{\Delta}} f(\mathbf{W}, \boldsymbol{\Delta}) + g(\mathbf{W}, \boldsymbol{\Delta}) + h(\mathbf{L}(\boldsymbol{\Delta}, \mathbf{W})), \quad (7)$$

where h incorporates the signal log-likelihood and the graph filter from Equation (3), which we apply to the tensor $\mathbf{L}(\boldsymbol{\Delta}, \mathbf{W}) \in \mathbb{R}^{T \times N \times N}$ that stacks instantaneous Laplacians.

The original PDS is a first-order algorithm to solve minimization problems of the following form

$$\arg \min_{\mathbf{x} \in \mathbb{R}^N} f(\mathbf{x}) + g(\mathbf{x}) + h(\mathbf{A}\mathbf{x}), \quad (8)$$

which, except for the last term, corresponds to our objective in Equation (7). The limitation of PDS is that $\mathbf{A} : \mathbb{R}^N \rightarrow \mathbb{R}^M$

Algorithm 1: Bilinear Primal-Dual Splitting (BiPDS)

Input: Step parameters $\tau_w, \tau_c, \sigma \geq 0$, initial estimates $(\mathbf{W}_0, \mathbf{\Delta}_0, \mathbf{Y}_0)$, maximum number of iterations N_{max}

Output: Estimated solution of Equation (7)

```

1 for  $n = 0$  to  $N_{max} - 1$  do
2    $\mathbf{W}_{n+1} \leftarrow$ 
     prox  $(\mathbf{W}_n - \tau_w (\mathbf{L}^{**}(\mathbf{\Delta}_n, \mathbf{Y}_n) + \nabla f_w(\mathbf{W}_n)))$ ;
      $\tau_w g_w$ 
3    $\mathbf{\Delta}_{n+1} \leftarrow$ 
     prox  $(\mathbf{\Delta}_n - \tau_c (\mathbf{L}^*(\mathbf{Y}_n, \mathbf{W}_n) + \nabla f_c(\mathbf{\Delta}_n)))$ ;
      $\tau_c g_c$ 
4    $\mathbf{Y}_{n+1} \leftarrow$ 
     prox  $(\mathbf{Y}_n + \sigma \mathbf{L}(2\mathbf{\Delta}_{n+1} - \mathbf{\Delta}_n, 2\mathbf{W}_{n+1} - \mathbf{W}_n))$ ;
      $\sigma h^*$ 
5   if converged then
6     break
7 return  $\mathbf{W}_{n+1}, \mathbf{\Delta}_{n+1}$ 

```

has to be a linear operator on \mathbf{x} , while our \mathbf{L} is a bilinear operator combining $\mathbf{\Delta}$ and \mathbf{W} , for which we need to design a specific method.

PDS looks for solutions to both a primal and a dual problem, given respectively by \mathbf{x} and $\mathbf{A}\mathbf{x}$, and iteratively brings them closer by combining gradient and proximal descent [17]. More precisely, given proximal parameters $\tau, \sigma > 0$, and an initial estimate $(\mathbf{x}_0, \mathbf{y}_0) \in \mathbb{R}^N \times \mathbb{R}^M$, it performs the following iteration for every $n \geq 0$, until convergence:

$$\mathbf{x}_{n+1} \leftarrow \text{prox}_{\tau g}(\mathbf{x}_n - \tau(\nabla f(\mathbf{x}_n) + \mathbf{A}^* \mathbf{y}_n)), \quad (9a)$$

$$\mathbf{y}_{n+1} \leftarrow \text{prox}_{\sigma h^*}(\mathbf{y}_n + \sigma \mathbf{A}(2\mathbf{x}_{n+1} - \mathbf{x}_n)), \quad (9b)$$

where \mathbf{A}^* is the adjoint of \mathbf{A} , and h^* is the Fenchel conjugate of the function h .

The main challenge of our setting comes from optimizing jointly for \mathbf{W} and $\mathbf{\Delta}$ the function h , composed with the graph filter k . With the separation and parallel update of the primal variables \mathbf{W}_n and $\mathbf{\Delta}_n$, we define Bilinear Primal-Dual Splitting in Algorithm 1. We note that the update of the dual variable \mathbf{Y}_n in Algorithm 1 corresponds to the one in Equation (9b), with operator \mathbf{A} substituted by the bilinear one \mathbf{L} .

To generalize PDS, we define the dual variable using the bilinear form $\mathbf{Y} = \mathbf{L}(\mathbf{\Delta}, \mathbf{W})$. Then, we observe that the primal update in Equation (9) relies on the adjoint of the linear operator \mathbf{A}^* , which maps the dual variable to the space of the primal one. In Equation (7), supposing that g and f are separable in the primal variables \mathbf{W} and $\mathbf{\Delta}$, we can define two update steps, each using the partial adjoints of \mathbf{L} [4], that we show to be

$$\begin{aligned} \mathbf{L}^*(\mathbf{Y}, \mathbf{W}) &= \mathbf{W} d\mathbf{Y}^\top, \\ \mathbf{L}^{**}(\mathbf{\Delta}, \mathbf{Y}) &= \mathbf{\Delta}^\top d\mathbf{Y}, \end{aligned} \quad (10)$$

where $d\mathbf{Y} \in \mathbb{R}^{T \times E}$ is the tensor whose entries are given by

$$[d\mathbf{Y}]_{t\epsilon nm} = Y_{t\epsilon nn} + Y_{t\epsilon mm} - Y_{t\epsilon nm} - Y_{t\epsilon mn}. \quad (11)$$

In the notation from Arens [4], we let A, B, C be normed linear spaces on \mathbb{R} , and we denote their dual and double dual

spaces by \cdot^* and \cdot^{**} respectively. Given a bilinear operator $\mathbf{L} : A \times B \rightarrow C$, its adjoints should satisfy

$$\begin{aligned} \mathbf{L}^* : C^* \times A &\rightarrow B^*, \\ \mathbf{L}^*(\mathbf{f}, \mathbf{x})(\mathbf{y}) &= \mathbf{f}(\mathbf{L}(\mathbf{x}, \mathbf{y})); \\ \mathbf{L}^{**} : B^{**} \times C^* &\rightarrow A^*, \\ \mathbf{L}^{**}(\mathbf{y}, \mathbf{f})(\mathbf{x}) &= \mathbf{f}(\mathbf{L}(\mathbf{x}, \mathbf{y})). \end{aligned} \quad (12)$$

$$(13)$$

In our case, the bilinear operator $\mathbf{L} : \mathcal{A} \times \mathcal{W} \rightarrow \mathcal{L}_T$ is defined as

$$\begin{aligned} [\mathbf{L}(\mathbf{\Delta}, \mathbf{W})]_{tnm} &= [\mathbf{L}_{\mathbf{\Delta}^\top \mathbf{W}}]_{tnm} \\ &= \begin{cases} -\sum_k \delta_{kt} w_{k(n,m)} & n \neq m, \\ \sum_k \delta_{kt} \sum_l w_{k(n,l)} & n = m, \end{cases} \end{aligned} \quad (14)$$

and it maps from the spaces of atom coefficients $\mathcal{A} = [0, 1]^{K \times T}$ and graph weights $\mathcal{W} = \mathbb{R}_+^{K \times E}$ to that of instantaneous Laplacians $\mathcal{L}_T \subset \mathbb{R}^{T \times N \times N}$.

We obtain the adjoint operators by solving the identities 12, 13 for the standard dot products of the given spaces. Starting from the adjoint operator with respect to weights, $\mathbf{L}^* : \mathbb{R}^{T \times N \times N} \times [0, 1]^{K \times T} \rightarrow \mathbb{R}_+^{K \times E}$, we observe

$$\langle \mathbf{Y}, \mathbf{L}(\mathbf{\Delta}, \mathbf{W}) \rangle = \sum_{tnm} Y_{tnm} [\mathbf{L}_{\mathbf{\Delta}^\top \mathbf{W}}]_{tnm} \quad (15a)$$

$$\begin{aligned} &= \sum_{tnm, n \neq m} Y_{tnm} \sum_k \delta_{kt} (-w_{k(n,m)}) \\ &\quad + \sum_{tn} Y_{tnn} \sum_k \delta_{kt} \sum_l w_{k(n,l)} \end{aligned} \quad (15b)$$

$$= \sum_{\substack{k(n,m) \\ n < m}} w_{k(n,m)} \left(-\sum_t \delta_{kt} (Y_{t\epsilon nn} + Y_{t\epsilon mm}) \right) \quad (15c)$$

$$\begin{aligned} &\quad + \sum_{k(n,l)} w_{k(n,l)} \sum_t \delta_{kt} Y_{t\epsilon nn} \\ &= \sum_{\substack{k(n,m) \\ n < m}} w_{k(n,m)} \sum_t \delta_{kt} (Y_{t\epsilon nn} + Y_{t\epsilon mm} - Y_{t\epsilon nm} - Y_{t\epsilon mn}) \end{aligned} \quad (15d)$$

$$= \left\langle \mathbf{W}, \mathbf{\Delta} \underbrace{[Y_{t\epsilon nn} + Y_{t\epsilon mm} - Y_{t\epsilon nm} - Y_{t\epsilon mn}]_{k(n,m)}}_{=d\mathbf{Y}} \right\rangle \quad (15e)$$

$$= \langle \mathbf{W}, \mathbf{L}^*(\mathbf{Y}, \mathbf{\Delta}) \rangle, \quad (15f)$$

where between Equation (15c) and Equation (15d) we split the second sum into two sums over directed edges

$$\sum_{k(n,l)} = \sum_{k(n,l), n < l} + \sum_{k(n,l), l < n}.$$

On the other hand, for the adjoint operator with respect to coefficients, $\mathbf{L}^{**} : \mathbb{R}_+^{K \times E} \times \mathbb{R}^{T \times N \times N} \rightarrow [0, 1]^{K \times T}$, we can follow the previous derivation until Equation (15d), then isolate the coefficient matrix and obtain

$$\langle \mathbf{\Delta}, \mathbf{L}^{**}(\mathbf{W}, \mathbf{Y}) \rangle = \left\langle \mathbf{\Delta}, \mathbf{W} d\mathbf{Y}^\top \right\rangle. \quad (16)$$

V. PRACTICAL MODELS

In this section we design some loss functions that we can optimize using Algorithm 1. We leverage the most common hypotheses from graph structure learning and sparse representation literature to expand on the negative log-likelihood of the general model from Equation (6):

$$\arg \min_{\mathbf{W}, \Delta} \ell_w(\mathbf{W}) + \ell_c(\Delta) + \ell_x(\mathbf{X}, \mathbf{W}, \Delta),$$

then we explicitly provide the terms for Equation (7) and derive their update steps for BiPDS. We conclude with a complexity analysis of these models and their optimization with Algorithm 1.

A. Objective function

We start by defining the following base objective, with regularization hyperparameters α 's:

$$\ell_w(\mathbf{W}) = \chi_{\mathbf{W} \geq 0} + \alpha_w L_1 \|\mathbf{W}\|_1 + \alpha_\perp \sum_{k' \neq k}^K \langle \mathbf{w}_k, \mathbf{w}_{k'} \rangle, \quad (17a)$$

$$\ell_c(\Delta) = \chi_{\Delta \in [0,1]} + \alpha_c L_1 \|\Delta\|_1, \quad (17b)$$

$$\ell_x(\Delta, \mathbf{W}) = \sum_{t=1}^T (\mathbf{x}_t^\top \mathbf{L}(\delta_t, \mathbf{W}) \mathbf{x}_t + h(\mathbf{L}(\delta_t, \mathbf{W}))). \quad (17c)$$

The first terms in both ℓ_w and ℓ_c include the domain constraints on \mathbf{W} and Δ , expressed as characteristic functions $\chi_{\mathbb{R}_+^{K \times E}}$ and $\chi_{[0,1]^{K \times T}}$ respectively, with

$$\chi_A(\mathbf{x}) = \begin{cases} 0 & \mathbf{x} \in A; \\ +\infty & \mathbf{x} \notin A. \end{cases} \quad (18)$$

The second terms of Equations (17a) and (17b) are weighted L_1 -norms that promote sparsity in the atom weights and in their coefficients respectively. They arise from n -variate exponential priors [18] on the entries of \mathbf{W} and Δ ,

$$P(\mathbf{y}) = \left(\frac{\alpha}{2}\right)^n \exp\left(-\frac{\alpha}{2} \mathbf{1}^\top \mathbf{y}\right), \quad (19)$$

with \mathbf{y} representing either atom weights or coefficients, and n being the corresponding number of entries. The third term in ℓ_w penalizes dot products across atom weights, which promotes orthogonality and, since we also require the matrix to have nonnegative entries, this regularization encourages edges to be zero if they are already present in another atom.

In Equation (17c), the first term in the sum measures total variation of each signal on the Laplacians of instantaneous graphs, and is minimized by structures on which signals are smooth. It corresponds to defining the prior signal distribution from Equation (3) on the graph filter $k(\Lambda) = \sqrt{\Lambda^\dagger}$, with \dagger denoting the Moore-Penrose pseudo-inverse. This signal distribution is known as Laplacian-constrained Gaussian Markov Random Field (LGMRF) [19]:

$$(\mathbf{x}_t | \mathbf{L}_t) = \frac{\exp\left(-\frac{1}{2} \mathbf{x}_t^\top \mathbf{L}_t \mathbf{x}_t\right)}{\sqrt{(2\pi)^N \det_+(\mathbf{L}_t^\dagger)}}, \quad (20)$$

where \det_+ represents the pseudo-determinant [20].

Finally, the function h describes additional hypotheses on instantaneous Laplacians, and in this work we propose two variants which give rise to the *GraphDictLog* and *GraphDictSpectral* models, which share the same objectives for ℓ_w and ℓ_c , and signal smoothness. The *GraphDictLog* model enforces node degrees to be positive for each instantaneous graph G_t using a log barrier on the diagonal of the Laplacians, as done by Kalofolias [21] and derivative works:

$$h(\mathbf{L}_t) = \mathbf{1}_N^\top \log(\text{diag}(\mathbf{L}_t)). \quad (21)$$

This formulation is more popular than using the logarithm of $\det_+(\mathbf{L}_t)$, which arises from Equation (20), as it is more computationally efficient and less prone to numerical issues.

The *GraphDictSpectral* model introduces a constraint that enforces all Laplacians to share the same eigenvectors \mathbf{U} , so that atoms represent filters on the same graph, instead of independent structures, since $k(\mathbf{L}_t) = \mathbf{U}k(\sum_k \delta_{kt} \Lambda_k) \mathbf{U}^\top$. This formulation corresponds to the model proposed by Thanou et al. [9]. We initialize \mathbf{U} with the eigendecomposition of the empirical covariance matrix [22], so that the optimization is only performed on atoms eigenvalues and coefficients. The specific h term enforces this constraint with a characteristic function χ , and includes the log barrier on the Laplacians pseudo-determinants [20] from the LGMRF prior:

$$h(\mathbf{L}_t) = \chi_{\mathbf{U} \Lambda_t \mathbf{U}^\top}(\mathbf{L}_t) + \log \det_+(\mathbf{L}_t). \quad (22)$$

Equations (17a) to (17c) are all sums of proximal and differentiable functions, and thus are compatible with Equation (7).

B. Implementation

In this section we present the proximal operators and gradients corresponding to the GraphDict objective proposed above, namely in Equations (17a) to (17c), (21) and (22). In short, signals and dictionaries are bound by the smoothness term in Equation (17c), then we promote sparsity by L1 regularization for both coefficients and weights, and for the latter we additionally introduce an orthogonality constraint. We regularize instantaneous Laplacians with either the log barrier on their diagonal from Equation (21), or with the log pseudo-determinant from Equation (22)

We start by providing an alternative formulation for the smoothness term in Equation (17c)

$$\begin{aligned} \sum_{t=1}^T \mathbf{x}_t^\top \mathbf{L}(\delta_t, \mathbf{W}) \mathbf{x}_t &= \sum_{t,k} \delta_{tk} \mathbf{x}_t^\top \mathbf{L}_{w_k} \mathbf{x}_t \\ &= \sum_{t,k} \sum_{n=1}^N \sum_{m=1}^N \delta_{tk} x_{tn} x_{tm} [\mathbf{L}_{w_k}]_{nm} \\ &= \sum_{t,k} \sum_{n=1}^N \delta_{tk} \left(\sum_{l \neq n}^N x_{tn}^2 w_{k(n,l)} - \sum_{m \neq n}^N x_{tn} x_{nm} w_{k(n,m)} \right) \\ &= \sum_{t,k} \sum_{(n,m) \in E} \delta_{tk} w_{k(n,m)} (x_{tn} - x_{tm})^2 \\ &= \|\Delta \mathbf{W} \odot \mathbf{Z}\|_1, \end{aligned} \quad (23)$$

where in the last line we introduce the matrix $\mathbf{Z} \in \mathbb{R}^{T \times E}$ of squared pairwise differences over edges, with entries $[\mathbf{Z}]_{t(n,m)} = (x_{tn} - x_{tm})^2$. For the second-to-last equality, we split the sum over pairs of nodes into two sums over directed edges. We remark that this formulation is equivalent to the one proposed by Kalofolias [21] to express signal smoothness over a single graph through pairwise node distances.

Putting together Equations (17a) to (17c) with the smoothness formulation above, our full objective for the experimental setup is

$$\arg \min_{\mathbf{W}, \Delta} g_w(\mathbf{W}) + g_c(\Delta) + f(\mathbf{W}, \Delta) + h(\mathbf{L}(\Delta, \mathbf{W})), \quad (24)$$

where

$$\begin{aligned} g_w(\mathbf{W}) &= \chi_{\mathbf{W} \geq 0} + \alpha_w L_1 \|\mathbf{W}\|_1 \\ g_c(\Delta) &= \chi_{\Delta \in [0,1]} + \alpha_c L_1 \|\Delta\|_1 \\ f(\mathbf{W}, \Delta) &= \|\Delta \mathbf{W} \odot \mathbf{Z}\|_1 + \alpha_\perp \sum_{k' \neq k}^K \langle \mathbf{w}_k, \mathbf{w}_{k'} \rangle, \end{aligned} \quad (25)$$

where g_w and g_c are proximable and f is sub-differentiable. The gradients of f with respect to our variables $\mathbf{W} \in \mathbb{R}_+^{K \times E}$ and $\Delta \in \mathbb{R}^{T \times K}$ are respectively

$$\begin{aligned} \nabla_{\mathbf{W}} f(\mathbf{W}, \Delta) &= \Delta^\top \mathbf{Z} + \alpha_\perp (\mathbf{1}\mathbf{1}^\top - \mathbf{I}_K) \mathbf{W}, \\ \nabla_{\Delta} f(\mathbf{W}, \Delta) &= \mathbf{Z} \mathbf{W}^\top. \end{aligned} \quad (26)$$

The proximal operators of g_w and g_c are

$$\text{prox}_{\tau_w g_w}(\mathbf{W}) = (\mathbf{W} - \tau_w \alpha_w L_1)_+, \quad (28)$$

$$\text{prox}_{\tau_c g_c}(\Delta) = (\Delta - \tau_c \alpha_c L_1)_{[0,1]}, \quad (29)$$

where in Equation (28) the function $(\mathbf{x})_+ = \max(\mathbf{x}, 0)$ is applied element-wise, as in Equation (29) for $(\mathbf{x})_{[0,1]} = \max(\min(\mathbf{x}, 1), 0)$.

For the function h , we have two different settings, for which we compute the Fenchel conjugate h^* . In the *GraphDictLog* case, we use the function from Equation (21), which sums the logarithms of node degrees for each instantaneous graph. For this setting, we do not need to pass through the Laplacian, as we only need the degree vectors of instantaneous graphs, which we can compute with the linear operator $\mathbf{D} \in \mathbb{R}^{N \times E}$ defined as

$$[\mathbf{D}\mathbf{w}]_n = \sum_{m \neq n} w_{(n,m)} \quad (30)$$

The dual term is therefore $\mathbf{Y} = \mathbf{D}(\Delta, \mathbf{W}) = \mathbf{D}(\Delta \mathbf{W})^\top \in \mathbb{R}^{N \times T}$, for which we have the two partial adjoints

$$\begin{aligned} \mathbf{D}^*(\mathbf{Y}, \mathbf{W}) &= \mathbf{Y}^\top \mathbf{D} \mathbf{W}^\top, \\ \mathbf{D}^{**}(\Delta, \mathbf{Y}) &= \Delta^\top \mathbf{Y} \mathbf{D}. \end{aligned} \quad (31)$$

Finally, the proximal operator of the Fenchel conjugate of h is

$$\text{prox}_{\sigma h^*}(\mathbf{Y}) = \frac{\mathbf{Y} - \sqrt{\mathbf{Y}^2 + 4\sigma}}{2}. \quad (32)$$

On the other hand, for *GraphDictSpectral*, we use the main formulation for $\mathbf{Y} = \mathbf{L}(\Delta, \mathbf{W})$ and the function h from

Equation (22). Fixing the eigenvectors for all Laplacians to be $\mathbf{U} \in \mathbb{R}^{N \times N}$, the proximal operator of h^* is

$$[\text{prox}_{\sigma h^*}(\mathbf{Y})]_t = \mathbf{U} \left(\frac{\Lambda_t - \sqrt{\Lambda_t^2 + 4\sigma \mathbf{I}_N}}{2} \right) \mathbf{U}^\top, \quad (33)$$

where, Λ_t are the eigenvalues each *instantaneous Laplacian* \mathbf{Y}_t in the tensor \mathbf{Y} ; the square root is applied component-wise on the diagonal and the identity is broadcasted as needed.

C. Complexity analysis

We study the computational complexity of optimizing *GraphDictLog* and *GraphDictSpectral* with Algorithm 1, with respect to the number of nodes N , the number of atoms K , the number of samples T , and the maximum number of iterations of BiPDS M .

Starting from *GraphDictLog*, we observe that the partial derivatives of f , in Equations (26) and (27) are dominated by matrix multiplications of complexity $\mathcal{O}(TKE)$, where E is the number of edges, which is in $\mathcal{O}(N^2)$. Computing the partial adjoint operators from Equation (31) is in $\mathcal{O}(TNEK)$. As the proximal operators in Equations (28) and (29) have complexity of $\mathcal{O}(KE)$ and $\mathcal{O}(TK)$ respectively, the updates of both \mathbf{W}_n and Δ_n are dominated by the adjoint computation from the dual variable. In the dual update, we have the bilinear computation $\mathbf{Y} = \mathbf{D} \mathbf{W}^\top \Delta^\top$ which has complexity of $\mathcal{O}(TKNE)$, and the proximal update from Equation (32) which is in $\mathcal{O}(NT)$. Therefore, each iteration of Algorithm 1 for optimizing *GraphDictLog* parameters has a complexity of $\mathcal{O}(TNEK)$, which cumulates to $\mathcal{O}(MTNEK)$, or $\mathcal{O}(MTN^3K)$ for dense graphs.

For *GraphDictSpectral*, we can leverage the fixed eigenvectors to reformulate the problem in the spectral space and greatly reduce computational complexity. More precisely, by taking the graph Fourier transform $\hat{\mathbf{X}} \mathbf{U}^\top$ of signals \mathbf{X} , we can reformulate Equation (17c) to only depend on the sparse diagonal matrix of Laplacians eigenvalues. This allows us to avoid computing eigendecompositions at each iteration, and therefore complexity is again dominated by computing the adjoint from the dual space to weights. The overall computational cost of Algorithm 1 for *GraphDictSpectral* is again $\mathcal{O}(MTNEK)$.

VI. EXPERIMENTS

We present three experiments to illustrate the capabilities of our GraphDict models. First, we show their ability to reconstruct superposed graphs from synthetic signals, outperforming state-of-the-art clustering methods. Second, we demonstrate their effectiveness in recovering time-varying graphs from sequential data, where they surpass dedicated temporal models. Finally, we apply them to a real-world EEG dataset to learn explainable brain states for a motor imagery classification task, achieving superior performance with fewer features than methods from the neuroscientific literature.

A. Superposing Graphs

1) *Description*: In this experiment we generate data according to the Graph-Dictionary Signal Model from Section III, and we focus on recovering *instantaneous* graphs. In particular, we investigate the evolution of model performances with respect to the maximum number of atoms that can contribute to each signal, which we call *superposition*. With a superposition of one, each signal arises from a single network and the problem is equivalent to signal clustering and graph reconstruction. Therefore, we compare GraphDictLog and GraphDictSpectral to *Gaussian Mixtures*—where we estimate the graph as the pseudo-inverse of the empirical correlation—*KGraphs* [13], and *GLMM* [12], as these methods are state of the art for the latter problem, but no model exists for higher superpositions. We re-implement the two latter, and we use Gaussian Mixtures from Scikit-learn [23].

2) *Data*: We sample a dictionary of $K = 5$ graphs from an Erdős-Renyi distribution with 30 nodes and $p = 0.2$ edge probability (ER(30,0.2)), which is shared by the following generation steps. Then, we define the *superposition* parameter $s \in \{1, \dots, 5\}$, that indicates the maximum number of atom coefficients that can be nonzero at the same time for each experiment run. Subsequently, for each $t \in \mathbb{N}$, we build a random coefficient vector δ_t by first sampling the number of positive coefficients uniformly from 1 to s , and then by randomly selecting the atoms. Figure 2 shows multiple sampled coefficients for each superposition value. We observe that, by definition, at most s atoms have nonzero coefficients, but some δ_t have less positive values.

We gather multiple independent samples from this process as columns of two matrices of discrete coefficients $\Delta_{tr} \in \{0, 1\}^{5 \times T_{tr}}$, $\Delta_{te} \in \{0, 1\}^{5 \times T_{te}}$, and from the corresponding instantaneous graphs $\Delta_{tr|te} \mathbf{W}$ we sample two sets of signals \mathbf{X}_{tr} and \mathbf{X}_{te} following a Laplacian-constrained Gaussian Markov Random Field, or LGMRF [19]. In this model the combinatorial Laplacian corresponds the precision matrix of a Gaussian distribution, so that signals follow Equation (3) for the filter $k(\Lambda) = \sqrt{\Lambda^\dagger}$. We use \mathbf{X}_{tr} and \mathbf{X}_{te} respectively for training and testing the models. Each atom contributes to multiple instantaneous graphs as we allow for more superposition, so we balance the tasks by setting T_{tr} to allow for each atom to contribute to 500 samples on average. More precisely, for $s = 1, \dots, 5$ we have $T_{tr} = 2500, 1666, 1250, 1000, 833$; while the test set has a fixed size of $T_{te} = 500$.

3) *Results*: We focus on the ability of models to correctly recover edges, and we measure their performances with the Matthews correlation coefficient (MCC) score:

$$MCC = \frac{tp \times tn - fp \times fn}{\sqrt{(tp + fp)(tp + fn)(tn + fp)(tn + fn)}}, \quad (34)$$

which takes into account true (t) and false (p) positive (p) and negative (n) edges. This metric, which takes values in the $[-1, 1]$ interval, is better suited than the F1 score in comparing edges presence or absence in sparse graphs, thanks to being balanced even with classes of very different sizes. For every graph-learning method, we perform a hyperparameter grid search by training on \mathbf{X}_{tr} and scoring on the instantaneous graphs of the same training set.

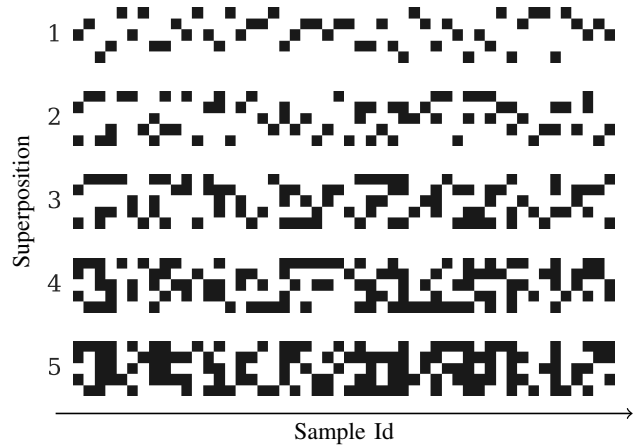


Fig. 2. Samples of coefficient matrices for different *superposition* values. Each block represents in black the positive coefficients of five atoms over 50 samples.

Figure 3 shows the evolution of the MCC, precision, and recall scores on the test set for increasingly superposed coefficients, averaged on five different random seeds. For a superposition value of 1, which corresponds to signal clustering, all graph learning methods perform similarly, while Gaussian Mixtures lag behind. With increasingly superposed graphs, GraphDictLog consistently provides the best results in terms of MCC. The overall high recall shows that all models, except GraphDictSpectral, recover too many edges. Furthermore, all precision curves increase with more atoms being superposed, in spite of the higher degrees of freedom of instantaneous graphs. Focusing on our GraphDictLog model, we observe that in this setting, with the low edge probability in the ER graphs, the most useful prior is sparsity on atom weights, from Equation (17a), controlled by α_{wL_1} .

B. Time-Varying Graphs

1) *Description*: In this experiment, we observe signals sequentially, as time series, and we aim to recover the underlying instantaneous graphs, which have temporal dependencies. Multiple models have been proposed for these settings, introducing priors on the evolution of networks over time, and we can have a fair comparison with three different benchmarks. First, *WindowLogModel* is a temporal version of the static graph-learning method from Kalofolias and Perraudin [24], which learns independent graphs over sliding windows. *TGFA* is a dynamic graph-learning paradigm encompassing the models from Kalofolias et al. [25] and Yamada et al. [26], which adds an L1 or L2 regularization on edge changes between adjacent windows to the WindowLogModel objective.

Yamada and Tanaka [27] take a different approach and suppose that the time-varying graphs can be represented in a hierarchical manner. They organize windows as a binary tree, with neighbors sharing parents, and assign learnable graphs to this hierarchy. The signal distribution within each window is characterized by an instantaneous network given by the sum of all graphs from the root to the corresponding leaf, so that the hierarchical graphs can be estimated with a

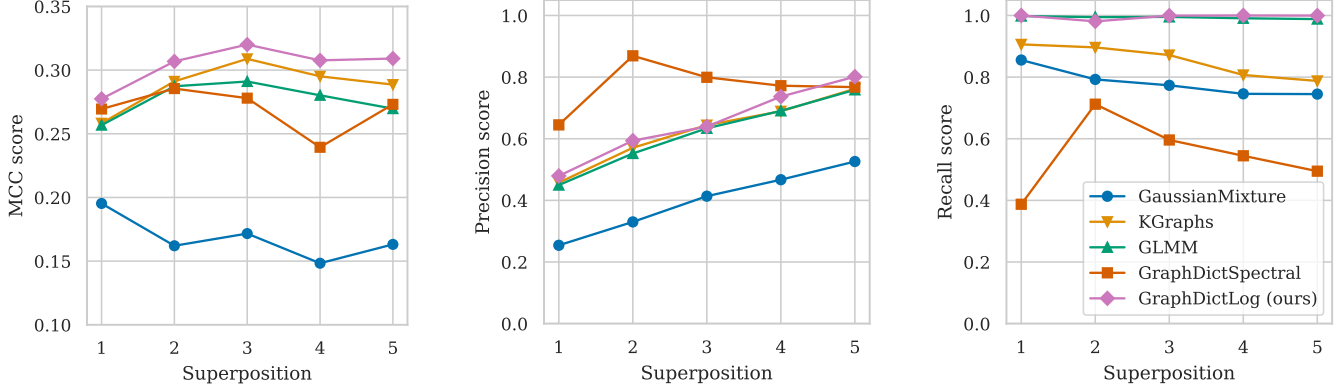


Fig. 3. Test performance on edge recovery of instantaneous graphs from signals, measured by Matthews correlation coefficient (MCC), precision and recall. Results are averaged over five random seeds.

TABLE I

EDGE RECOVERY PERFORMANCES, MEASURED BY AVERAGE MCC SCORE ACROSS ALL INSTANTANEOUS GRAPHS, FOR THE TIME SERIES EXPERIMENTS. EACH STOCHASTIC MODEL IS RANDOMLY INITIALIZED MULTIPLE TIMES, AND WE REPORT ITS AVERAGE SCORE AND STANDARD DEVIATION.

Distribution	EMEG						SBG					
	32 · 20			512 · 1			32 · 20			512 · 1		
Metric	MCC	Prec	Rec	MCC	Prec	Rec	MCC	Prec	Rec	MCC	Prec	Rec
WindowLogModel	37.7	35.6	55.7	36.0	37.9	51.2	33.6	22.6	66.9	28.6	16.4	72.3
TGFA	20.7	16.5	63.0	17.8	15.4	86.5	14.0	8.7	69.7	15.7	8.5	74.1
GraphDictHier	50.6 ± 0.4	36.6 ± 1.2	87.8 ± 2.1	40.2 ± 0.9	30.8 ± 1.4	80.8 ± 1.9	32.8 ± 2.1	19.7 ± 1.9	76.5 ± 0.8	31.2 ± 0.3	17.9 ± 0.1	75.5 ± 0.2
GraphDictSpectral	57.2 ± 6.7	52.8 ± 11.6	71.6 ± 3.3	26.9 ± 0.7	40.2 ± 3.3	27.7 ± 4.6	29.6 ± 1.5	16.3 ± 0.5	81.6 ± 3.3	18.4 ± 0.7	22.3 ± 6.6	27.1 ± 12.0
GraphDictLog	61.0 ± 1.6	86.2 ± 1.8	46.7 ± 2.5	46.2 ± 2.0	58.4 ± 4.0	43.9 ± 4.0	48.1 ± 1.1	40.7 ± 1.4	64.7 ± 0.6	44.0 ± 2.2	39.8 ± 3.0	52.1 ± 2.7

maximum likelihood formulation. Due to its additive nature, this model falls within our dictionary framework, with graphs in the hierarchy corresponding to atoms, but with a substantial difference in the coefficients. In their case, these are fixed and describe the tree structure, while in the dictionary learning setting they are parameters of the model. We implement this hierarchical graph-learning model as *GraphDictHier*, by fixing the atoms coefficients and only learning atom edge weights.

For this experiment, we include a temporal prior in *GraphDictLog* and *GraphDictSpectral*, similarly to *TGFA*, by introducing an L_1 regularization on the difference in coefficients of adjacent windows to Equation (17b) to promote sparsity in changes

$$\alpha_{\text{diff}} \sum_{t=1}^{T-1} \|\delta_{t+1} - \delta_t\|_1. \quad (35)$$

This term encourages atom coefficients to be constant between t and $t + 1$, or to change abruptly. We also allow for coefficients to be fixed over windows, with the size becoming a hyperparameter with the same search space as benchmarks.

2) *Data*: We generate sequential graphs from two time-varying distributions, which we use in separate runs:

- The *Edge-Markovian evolving graph* (EMEG) model starts with a sample of $\text{ER}(36, 0.1)$, and at each graph change we add new edges or remove existing ones from the current network with probabilities of 0.001 and 0.01 respectively.

- The *Switching behavior graph* (SBG) model consists of six independent $\text{ER}(36, 0.05)$ networks, that define states in a Markov Process. At each step we either keep the same graph as the previous one, with probability of 0.98, or change uniformly to another one.

In both models, weights for new edges are sampled uniformly on the $[0.1, 3]$ interval, and do not change until the edge disappears. With these models we obtain sequences of T_G weights $W \in \mathbb{R}_+^{T_G \times E}$, that allow us to sample signals from the LGMR distribution presented in Section VI-A2. For each time-varying graph process, we study two signal generation settings:

- 1) Graphs are stable over windows: we set $T_G = 32$, and we sample $W = 20$ consecutive signals $X_w \in \mathbb{R}^{W \times N}$, for a total of 640 measurements;
- 2) The system is continually evolving: we sample $T_G = 512$ graphs each of which produces a single signal $x_t \in \mathbb{R}^N$.

3) *Results*: Table I shows the performances in edge recovery of benchmarks and the different *GraphDict* models on all time series tasks, averaged over five random seeds. We select hyperparameters of every model by grid search and evaluation on training reconstruction. Including the additional regularization from Equation (35) in the loss term proved to be an effective prior for the EMEG process; while enforcing coefficients to change over windows instead of over samples improved reconstruction performances for the SBG process.

We see that our GraphDictLog greatly outperforms other methods in all settings, showing that it can capture the gradual evolution of the EMEG distribution, as well as the recurrent graphs of SBG. In particular, it achieves the highest precision in all scenarios, indicating that the recovered edges are more likely to be correct. However, the model exhibits a lower recall compared to other methods, which might suggest that the sparsity priors on weights and coefficients were too strong, despite hyperparameter tuning. We see that the scores of all models are consistently higher in the stable 32×20 setting, in particular thanks to the hypothesis of window-based models being correct. We suppose that the advantage over the hierarchical model from Yamada and Tanaka [27], which they presented as state of the art, comes from the greater flexibility of our model in learning on its own when atoms contribute to a sample, or window. In particular, for the SBG setting, in which states are recurrent, our model can “reuse” atoms across time, while the hierarchical model has less memory across windows far apart. This also explains why GraphDictHier shows a higher recall than GraphDictLog, as the consistency of neighboring samples might enforce to focus on fewer persistent edges.

C. Brain States For Motor Imagery

1) *Description*: In this final experiment we study the capability of GraphDict to learn an explainable representation for a downstream classification task, in particular in its GraphDict-Log form. We analyze brain activity measurements with the objective of disambiguating left and right-hand motor imagery. Neurologists often resort to *microstates* [28] to characterize brain signals, and they obtain such states by clustering EEG signals over time. This is an interesting setting for our model, where instead of single microstates we can reconstruct a dictionary of states (graph atoms) that can provide insights on brain connectivity.

We infer brain states as the clusters, or atoms, learned by GraphDictLog and three baseline methods: *KMeans*, which is the standard method for microstate inference; *Gaussian Mixtures*, which allow for soft assignments [29]; *GLMM*, that include network properties on states [30]. We perform the classification task on separate time windows, called *events*. For each event we compute three features for each state, based on the evolution of attribution probabilities, for clustering methods, and coefficients, for graph dictionaries:

- *Number of occurrences* (OCC): count of continuous intervals covered;
- *Coverage* (COV): total time over the window;
- *Average duration*: average length of continuous occurrences in seconds, i.e. OCC/COV.

2) *Data*: The data for this experiment consists in a set of annotated Electroencephalography (EEG) signals from the EEG BCI dataset [31], provided by the MNE-Python library [32]. EEGs are multivariate time series of electrical potentials captured by electrodes placed over the subjects scalp. This dataset collects measurements from 15 subjects, each with 45 *events* spanning the onset of imagined motion of either hand, with 23 for the left and 22 for the right hand.

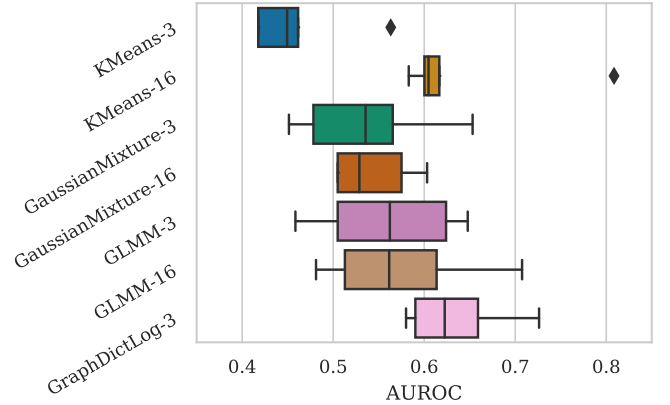


Fig. 4. Distribution of test scores for motor imagery classification from brain state features, computed by leave-one-subject-out cross-validation. On the y-axis we find the name of the model used for learning brain states, together with the number of clusters, or atoms, defining such states.

3) *Pipeline*: We preprocess the data according to microstates’ literature [28, 29] to obtain clean signals for the 64 EEG channels, from which we infer brain states and their relative features. The full pipeline consists in the following five steps, which we perform separately for every benchmark clustering model and our graph-dictionary learning one, with multiple hyperparameters each:

- 1) **Data preprocessing** according to Microstates literature:
 - a) We re-reference EEG signals and center each sample to the average over all electrodes

$$\mathbf{x}_t \leftarrow \mathbf{x}_t - \frac{1}{N} \sum_{n=1}^N \mathbf{x}_{tn}; \quad (36)$$

- b) We apply a band-pass filter between 0.5 and 30 Hz;
- 2) **State embedding**: we identify the “cleanest samples of brain activity”, which according to neurologists are peaks of the *Global Field Power* (GFP), which we use to identify brain states. More precisely:
 - a) We compute Global Field Power, which is the standard deviation across channels of each sample;
 - b) We identify the *peaks* of this series;
 - c) We train the given clustering or GraphDict model and retrieve cluster, or atom, assignments of peaks;
 - d) We assign to each samples in EEG events the same coefficients as its closest peak in time;
 - 3) **Feature extraction**: we compute the pre-cited state features for each EEG event;
 - 4) **Classification**: we train and test multiple random forest classifiers with leave-one-patient-out cross validation;

Finally, we gather the results for each state embedding model. We report the distribution of test scores on motor imagery classification corresponding to the best hyperparameters with the best downstream classifier.

4) *Results*: Figure 4 shows the results’ distribution of random forest classifiers on 15-fold cross validation, with each fold corresponding to a unique subject. For each method we test different numbers of states, or clusters, and select

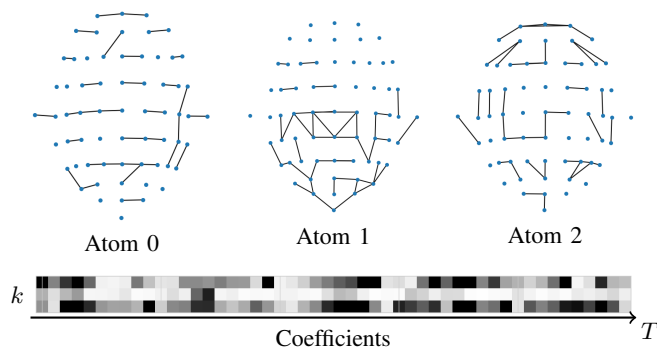


Fig. 5. Atoms and 50 corresponding coefficients learned by `GraphDictLog` on EEG signals from motor imagery data. Atoms are sorted by frequency of appearance and show edges between electrodes. The coefficient matrix is color coded from zero, in white, to one, in black, and has atoms as rows and sample indices as columns.

other hyperparameters to obtain the highest average training performance in classification. We see that `GraphDictLog` with three atoms obtains consistently the highest AUROC, with the only comparable model being `KMeans` with 16 clusters. Still, `KMeans-16` requires 48 features, against the nine features arising from the three states of `GraphDictLog-3`. Interestingly, of all regularization terms from Equations (17a) to (17c), only α_{\perp} , which enforces edge orthogonality, is positive.

In this setting, we observe a strong influence of the physics of the problem on the data, which translates in electrodes being close in space to be highly correlated due to the skull acting as a diffuser for brain activity. To avoid this strong correlation to take over, enforcing atom orthogonality proves to be an effective solution. The top of Figure 5 shows the reconstructed atoms corresponding to the best classification model, ordered by their average activation from low to high. We see many edges between electrodes close in space, but the atoms seem to capture functional areas, as we recognize the frontal lobe in Atom 1, and the increased connectivity of the occipital lobe in Atom 2 might correspond to visual activity. The bottom part of the figure shows the coefficients of the signals from 50 peaks of GFP, of which the first 28 are from the imagined movement of the right hand, and the rest from the left hand. Even though we cannot identify any meaningful pattern in the coefficients, we can examine feature importance in the random forest model, in terms of mean decrease in impurity. Interestingly, models focus almost entirely on the coefficient features corresponding to Atoms 1 and 2, each of which gets almost equal importance (≈ 0.16).

VII. CONCLUSION

We propose *GraphDict*, a Graph-Dictionary signal model for multivariate data, together with an optimization algorithm to jointly learn atoms and their coefficients. This framework characterizes systems with complex dynamics and provides novel insights on data, by reconstructing a dictionary of graphs that defines the probability distribution of the observed phenomena. Furthermore, our model provides sparse representations in the form of atom coefficients, which are inherently explainable as they describe the influence of the corresponding graph on the data generating process. Atom coefficients of our

GraphDict model are also shown to be relevant in downstream tasks, for instance to describe brain states for motor imagery classification problems.

Our formulation can also leverage expert knowledge, which we include as priors on signals, weights, and coefficients. In all applications, we observe that choosing well-thought priors significantly improves the model capabilities. More precisely, weight sparsity is very helpful when it reflects the ground truth graphs, as in our synthetic settings. For temporal data regularizing changes between activations over time helps capture the sequential aspect of the underlying process.

The expressive power of our framework comes with some limitations that open up several promising directions for future research. A first set of challenges relates to the specific instantiation of our model presented in Section V. While the general formulation in Equation (6) is highly flexible, our practical implementation relies on specific priors and regularization terms (e.g., α_{wL_1} , α_{cL_1} , α_{\perp}) that require heuristic tuning. The high computational complexity, also tied to this specific model, makes extensive hyperparameter search challenging. This is not an inherent limitation of the *GraphDict* framework itself, but rather of the chosen objective function. A key direction for future work is to explore other models within our framework, potentially with different regularizers or data fidelity terms that are more computationally efficient or allow for a more principled theoretical analysis of their impact on the estimated parameters.

Second, while our proposed BiPDS algorithm performs well empirically, a formal proof of its convergence remains an open theoretical question. Establishing convergence guarantees, perhaps under specific assumptions on the objective function, would be a significant contribution that would bolster the reliability of our method and could inspire other solutions for similar bilinear problems.

The generality of our framework opens up numerous other exciting extensions. The current model assumes a static dictionary, but it could be extended to allow atoms to evolve over time. Similarly, while we used an LGMRF model, the framework can readily incorporate other graph signal models. An ambitious but promising direction is to integrate principles from optimal transport, as discussed in Section II, to handle signals from graphs with non-aligned or varying node sets. These future explorations underscore the broad applicability and potential of our core contribution.

Thanks to the flexibility of *GraphDict* and its optimization algorithm to accommodate for different regularization terms and priors, this framework can leverage domain knowledge and provide insightful representations of multivariate data from different domains.

ACKNOWLEDGMENTS

This work was supported by the SNSF Sinergia project “PEDESITE: Personalized Detection of Epileptic Seizure in the Internet of Things (IoT) Era” under grant agreement CRSII5 193813.

REFERENCES

- [1] R. Rubinstein, A. M. Bruckstein, and M. Elad, "Dictionaries for Sparse Representation Modeling," *Proceedings of the IEEE*, vol. 98, no. 6, Jun. 2010. DOI: [10.1109/JPROC.2010.2040551](https://doi.org/10.1109/JPROC.2010.2040551)
- [2] X. Dong, D. Thanou, M. Rabbat, and P. Frossard, "Learning Graphs From Data: A Signal Representation Perspective," *IEEE Signal Processing Magazine*, vol. 36, no. 3, May 2019. DOI: [10.1109/MSP.2018.2887284](https://doi.org/10.1109/MSP.2018.2887284)
- [3] G. Mateos, S. Segarra, A. G. Marques, and A. Ribeiro, "Connecting the Dots: Identifying Network Structure via Graph Signal Processing," *IEEE Signal Processing Magazine*, vol. 36, no. 3, May 2019. DOI: [10.1109/MSP.2018.2890143](https://doi.org/10.1109/MSP.2018.2890143)
- [4] R. Arens, "The Adjoint of a Bilinear Operation," *Proceedings of the American Mathematical Society*, vol. 2, no. 6, 1951. DOI: [10.2307/2031695](https://doi.org/10.2307/2031695)
- [5] C. Vincent-Cuaz, T. Vayer, R. Flamary, M. Corneli, and N. Courty, "Online Graph Dictionary Learning," in *Proceedings of the 38th International Conference on Machine Learning*, PMLR, Jul. 2021.
- [6] W. Liu, J. Xie, C. Zhang, M. Yamada, N. Zheng, and H. Qian, "Robust Graph Dictionary Learning," in *The Eleventh International Conference on Learning Representations*, Sep. 2022.
- [7] Z. Zeng, R. Zhu, Y. Xia, H. Zeng, and H. Tong, "Generative Graph Dictionary Learning," in *Proceedings of the 40th International Conference on Machine Learning*, PMLR, Jul. 2023.
- [8] B. Das and E. Isufi, "Tensor Graph Decomposition for Temporal Networks," in *ICASSP 2024 - 2024 IEEE International Conference on Acoustics, Speech and Signal Processing (ICASSP)*, Apr. 2024. DOI: [10.1109/ICASSP48485.2024.10447234](https://doi.org/10.1109/ICASSP48485.2024.10447234)
- [9] D. Thanou, D. I. Shuman, and P. Frossard, "Parametric dictionary learning for graph signals," in *IEEE Global Conference on Signal and Information Processing*, Dec. 2013. DOI: [10.1109/GlobalSIP.2013.6736921](https://doi.org/10.1109/GlobalSIP.2013.6736921)
- [10] A. Karaaslanli and S. Aviyente, "Multiview Graph Learning With Consensus Graph," *IEEE Transactions on Signal and Information Processing over Networks*, vol. 11, 2025. DOI: [10.1109/TSIPN.2025.3527888](https://doi.org/10.1109/TSIPN.2025.3527888)
- [11] H. P. Margetic, M. E. Gheche, and P. Frossard, "Graph Heat Mixture Model Learning," in *Asilomar Conference on Signals, Systems, and Computers*, Oct. 2018. DOI: [10.1109/ACSSC.2018.8645150](https://doi.org/10.1109/ACSSC.2018.8645150)
- [12] H. P. Margetic and P. Frossard, "Graph Laplacian Mixture Model," *IEEE Transactions on Signal and Information Processing over Networks*, vol. 6, 2020. DOI: [10.1109/TSIPN.2020.2983139](https://doi.org/10.1109/TSIPN.2020.2983139)
- [13] H. Araghi, M. Sabbaqi, and M. Babaie-Zadeh, "\$K\$-Graphs: An Algorithm for Graph Signal Clustering and Multiple Graph Learning," *IEEE Signal Processing Letters*, vol. 26, no. 10, Oct. 2019. DOI: [10.1109/LSP.2019.2936665](https://doi.org/10.1109/LSP.2019.2936665)
- [14] A. Ortega, *Introduction to Graph Signal Processing*. Cambridge: Cambridge University Press, 2022. DOI: [10.1017/9781108552349](https://doi.org/10.1017/9781108552349)
- [15] A. Sandryhaila and J. M. F. Moura, "Discrete Signal Processing on Graphs," *IEEE Transactions on Signal Processing*, vol. 61, no. 7, Apr. 2013. DOI: [10.1109/TSP.2013.2238935](https://doi.org/10.1109/TSP.2013.2238935)
- [16] L. Condat, "A Primal–Dual Splitting Method for Convex Optimization Involving Lipschitzian, Proximable and Linear Composite Terms," *J Optim Theory Appl*, vol. 158, no. 2, Aug. 2013. DOI: [10.1007/s10957-012-0245-9](https://doi.org/10.1007/s10957-012-0245-9)
- [17] N. Parikh and S. Boyd, *Proximal Algorithms*. Now Publishers, Nov. 2013.
- [18] H. E. Egilmez, E. Pavez, and A. Ortega, "Graph Learning From Data Under Laplacian and Structural Constraints," *IEEE Journal of Selected Topics in Signal Processing*, vol. 11, no. 6, Sep. 2017. DOI: [10.1109/JSTSP.2017.2726975](https://doi.org/10.1109/JSTSP.2017.2726975)
- [19] H. E. Egilmez, E. Pavez, and A. Ortega, "Graph learning with Laplacian constraints: Modeling attractive Gaussian Markov random fields," in *Asilomar Conference on Signals, Systems and Computers*, Nov. 2016. DOI: [10.1109/ACSSC.2016.7869621](https://doi.org/10.1109/ACSSC.2016.7869621)
- [20] A. Holbrook, "Differentiating the pseudo determinant," *Linear Algebra and its Applications*, vol. 548, Jul. 2018. DOI: [10.1016/j.laa.2018.03.018](https://doi.org/10.1016/j.laa.2018.03.018)
- [21] V. Kalofolias, "How to Learn a Graph from Smooth Signals," in *International Conference on Artificial Intelligence and Statistics*, May 2016. DOI: [10.48550/arXiv.1601.02513](https://doi.org/10.48550/arXiv.1601.02513)
- [22] M. Navarro, Y. Wang, A. G. Marques, C. Uhler, and S. Segarra, "Joint Inference of Multiple Graphs from Matrix Polynomials," *Journal of Machine Learning Research*, vol. 23, no. 76, 2022.
- [23] F. Pedregosa et al., "Scikit-learn: Machine Learning in Python," *Journal of Machine Learning Research*, vol. 12, no. 85, 2011.
- [24] V. Kalofolias and N. Perraudin, "Large Scale Graph Learning From Smooth Signals," in *International Conference on Learning Representations*, Sep. 2018.
- [25] V. Kalofolias, A. Loukas, D. Thanou, and P. Frossard, "Learning time varying graphs," in *IEEE International Conference on Acoustics, Speech and Signal Processing (ICASSP)*, Mar. 2017. DOI: [10.1109/ICASSP.2017.7952672](https://doi.org/10.1109/ICASSP.2017.7952672)
- [26] K. Yamada, Y. Tanaka, and A. Ortega, *Time-Varying Graph Learning with Constraints on Graph Temporal Variation*, Jan. 2020. DOI: [10.48550/arXiv.2001.03346](https://doi.org/10.48550/arXiv.2001.03346)
- [27] K. Yamada and Y. Tanaka, "Temporal Multiresolution Graph Learning," *IEEE Access*, vol. 9, 2021. DOI: [10.1109/ACCESS.2021.3120994](https://doi.org/10.1109/ACCESS.2021.3120994)
- [28] C. M. Michel and T. Koenig, "EEG microstates as a tool for studying the temporal dynamics of whole-brain neuronal networks: A review," *NeuroImage, Brain Connectivity Dynamics*, vol. 180, Oct. 2018. DOI: [10.1016/j.neuroimage.2017.11.062](https://doi.org/10.1016/j.neuroimage.2017.11.062)

- [29] A. Mishra, B. Englitz, and M. X. Cohen, “EEG microstates as a continuous phenomenon,” *NeuroImage*, vol. 208, Mar. 2020. DOI: [10.1016/j.neuroimage.2019.116454](https://doi.org/10.1016/j.neuroimage.2019.116454)
- [30] I. Ricchi, A. Tarun, H. P. Margetic, P. Frossard, and D. Van De Ville, “Dynamics of functional network organization through graph mixture learning,” *NeuroImage*, vol. 252, May 2022. DOI: [10.1016/j.neuroimage.2022.119037](https://doi.org/10.1016/j.neuroimage.2022.119037)
- [31] G. Schalk, D. McFarland, T. Hinterberger, N. Birbaumer, and J. Wolpaw, “BCI2000: A general-purpose brain-computer interface (BCI) system,” *IEEE Transactions on Biomedical Engineering*, vol. 51, no. 6, Jun. 2004. DOI: [10.1109/TBME.2004.827072](https://doi.org/10.1109/TBME.2004.827072)
- [32] A. Gramfort et al., “MEG and EEG data analysis with MNE-Python,” *Front. Neurosci.*, vol. 7, Dec. 2013. DOI: [10.3389/fnins.2013.00267](https://doi.org/10.3389/fnins.2013.00267)